ENERGY SPECTRUM OF SPUTTERED URANIUM*

R. A. WELLER and T. A. TOMBRELLO

W. K. Kellogg Radiation Laboratory

California Institute of Technology, Pasadena, California 91125

*Supported in part by the National Science Foundation [PHY76-83685], the National Aeronautics and Space Administration [NGR 05-002-333], and the Energy Research and Development Administration [EX-76-G-03-1305].

ABSTRACT

The fission track technique for detecting ^{235}U has been used in conjunction with a mechanical time-of-flight spectrometer in order to measure the energy spectrum in the region 1 eV to 1 keV of material sputtered from a 93% enriched ^{235}U foil by 80 keV $^{40}Ar^{+}$ ions. The spectrum was found to exhibit a peak in the region 2-4 eV and to decrease approximately as $E^{-1.77}$ for $E \gtrsim 100$ eV. The design, construction and resolution of the mechanical spectrometer are discussed and comparisons are made between the data and the predictions of the random collision cascade model of sputtering.

1 INTRODUCTION

When a high velocity ion or atom strikes the surface of a solid target the collision may result in the ejection of atoms from the target material. From a macroscopic point of view, this process, known as sputtering, is reduced to a consideration of various aspects of the sputtering yield, S, which is the number of atoms of the target that are ejected per incident ion that strikes the surface. We shall here be concerned with the energy spectrum of the ejected particles, S(E), where E is the ejection energy.

As McCracken[1] has pointed out, the total sputtering yield has proved to be rather insensitive to the details of particular models of the sputtering process. Measurements of the energy distribution of the sputtered particles taken under various conditions have, therefore, been undertaken in the hope that the additional data will be more sensitive. Such measurements are difficult for two reasons: First, most of the ejected particles are neutral; second, they are quite low in energy, the most probable energy of ejection usually being between 1 eV and 10 eV. As a result, the experiments performed to date have been limited in the choices of either targets or bombardment conditions. One common type of experiment involves the post ejection ionization of the sputtered atoms followed by analysis. Typical examples are the experiments of Stuart and Wehner[2] and Stuart et al.[3] These experiments, which were carried out in a plasma, involved the observation of photons emitted from sputtered particles in a time-of-flight scheme. In the second experiment doppler shift measurements of the photons were also made. In another variation on this procedure Oechsner and Reichert[4] combined post-ionization and

retarding field analysis, and later Bernhardt et al.[5] used mass spectrometry as well. A second general class of experiments involves a time-of-flight technique to disperse the sputtered material on a collector, which is then analyzed by a sensitive technique to measure the quantity of deposited material. The most extensive set of sputtering measurements to date is of this type and is described by Thompson,[6] Farmery and Thompson,[7] Chapman et al.[8] and Reid et al.[9] All these experiments were carried out with an apparatus first described by Thompson et al.[10] Only copper and gold targets have been investigated by this method with gold being the more extensively studied. In these experiments sputtering was done by ions in the energy range > 10 keV and collected material measured by autoradiography. Our experiment is quite similar in form to these; however, time-of-flight or velocity selection experiments may differ in detail as evidenced by previous work described in the literature; e.g., Beuscher and Kipitzki,[11] Hulpke and Schlier,[12] and Politiek and Kistemaker.[13]

There were two main reasons for undertaking this work: (1) To provide additional data to better test theoretical models of the sputtering process. Considering the amount of work that has been done on all aspects of sputtering the amount of energy spectrum data available is small. Particularly lacking are the spectra of particles sputtered from compounds. The technique to be described here can be applied to the sputtering of uranium compounds almost as easily as it has here been applied to the sputtering of uranium metal. (2) The second motivation came from planetary science. Haff et al.[14] have shown that the sputtering of the lunar surface by the solar wind may lead to modification of the chemical and isotopic composition of the surfaces of lunar dust grains. In order to make predictions, however, it is necessary

to know the energy distribution of the sputtered atoms. While most data taken to date agree rather well with model predictions, there are nevertheless some systematic deviations. Furthermore, no reliable means is now at hand for predicting the energy distributions of the various component atoms sputtered from a heterogeneous target. The work completed is applied mainly to the first of these problems.

Part 2 of this paper describes the design and construction of the apparatus used in our experiment. Part 3 discusses the procedures followed in obtaining the data. In part 4 the data are presented along with an expanded discussion of the instrumental resolution and a comparison of the data with the model of Thompson.[6] Finally, part 5 contains a summary and our concluding remarks.

2 THE EXPERIMENTAL APPARATUS

A diagram of the apparatus used in this experiment is shown in Figure 1. The ion beam is produced in the 150 KV duoplasmatron ion source and is momentum selected by a 31^{o} magnet before entering the spectrometer chamber. There it passes through an arrangement of two fixed slits 1.11 cm wide by 0.45 cm high. Between these slits is the rim of a rapidly rotating disk with two diametrically opposed slits of the same size as the fixed slits. During each rotation of the disk each moving slit passes between the fixed slits allowing the ion beam to pass momentarily. The beam pulse so produced continues through a liquid nitrogen-filled cold trap into an ultra-high vacuum system (base pressure of $\approx 5 \times 10^{-10}$ Torr) where it strikes the target. Sputtered material ejected back in the direction of the beam, passes through one of the fixed slits and is collected on the rotating disk.

In addition to the fact that this geometry allows the velocity spectrum to be measured normal to the target surface, it has two practical advantages. First, since the beam pulse is caused by the moving collector there is no possibility for the beam pulses and the rotating collector to get out of synchronization. Second, the time zero of the collected spectrum is uniquely determined by the geometry of the disk.

The design considerations of the apparatus for this experiment are similar to those described by Thompson et al.[10] We consider a rotating collector of radius r, the rotation rate ν(rev/sec), at a distance ℓ from the target being sputtered. In the time, ℓ/v, that it takes a sputtered particle with velocity v to reach the collector the rim of the collector has rotated a linear distance of

$$x = \frac{2\pi r \ell \nu}{v} \equiv \frac{k}{v} . \qquad (1)$$

This equation defines the dispersion constant, k, whose value is a function of the apparatus design only. Like Thompson et al.[10] we also assume that the beam pulse is some fraction f of the period of rotation of the collector and that the width of the fixed slit which defines the trajectories of those sputtered particles which strike the collector is chosen to be $d = 2\pi rf$. Equating d and x gives an equation that may be viewed as defining the maximum velocity that can be resolved with a given apparatus or equivalently, as specifying the requirements that must be met by the apparatus to resolve a given velocity. The equation is

$$f\nu = \ell\nu . \qquad (2)$$

Before further consideration of this requirement, let us derive a condition

for the dispersion constant itself. It is obvious that the amount of dispersion required to obtain a satisfactory velocity spectrum on the collector is related to the spatial resolution of the technique that is used to measure the amount of collected material as a function of position. In practice, any technique will measure the amount of material in some region of width Δx at a position x on the collector. Thus, a reasonable criterion that must be satisfied is that the dispersion constant, k, be sufficiently large that the fractional change in v associated with the width Δx is below some specified tolerance for the maximum v to be studied. Taking the derivative of Equation (1), this condition is

$$\frac{|\Delta x| v_{max}}{\left|\frac{\Delta v}{v}\right|} \leq k \ . \tag{3}$$

We have chosen to design the apparatus to resolve 1 keV ^{235}U which have a velocity of 2.85×10^6 cm/sec. The $|\Delta x|$ associated with the nuclear track technique used to detect the sputtered ^{235}U is ≈ 0.02 cm. Picking 5% as a reasonable value of $|\Delta v/v|$ then requires that

$$k \gtrsim 1.14 \times 10^6 \text{ cm}^2/\text{sec}. \tag{4}$$

Returning now to the requirement (2):

$$fv \gtrsim 4.00 \times 10^4 \text{ cm/sec}, \tag{5}$$

where f has been chosen to be 1.4%. This choice is quite arbitrary at this point, although intuition suggests that a value around 1% is appropriate. (The precise effect that f has upon the final spectrum will be given in the discussion of the results of the experiment.) Since the density of

sputtered particles collected in a given time falls off as l^{-2}, it is clear from Equation (5) that ν should be chosen as large as practical. A motor was found that attains a speed of 500 rev/sec. Therefore, l was chosen to be $\approx$ 80 cm and as a result of (1) and (4), $r \gtrsim 4.5$ cm. In fact, r was chosen to be 5.08 cm giving the apparatus a dispersion constant of $k = 1.30 \times 10^6$ cm^2/sec.

One final factor that must be considered in the apparatus design is the constancy of the motor speed. In order that the inherently high spatial resolution of the nuclear track technique not be wasted, it is necessary to place an upper limit, ΔT, on the allowable fluctuation in the revolution period, T, of the motor. Thus

$$\frac{\Delta T}{T} \lesssim \frac{\Delta x}{2\pi r} \quad . \tag{6}$$

For a rate of rotation $\nu = 1/T = 500$ rev/sec,

$$\Delta T \lesssim 1.25 \ \mu\text{sec}$$

or

$$\frac{\Delta T}{T} \lesssim 0.05\%.$$

In addition, $\Delta\nu/\nu$ should also be $\lesssim 0.05\%$ instantaneously.

Where the load conditions may vary, the simplest way to meet the requirement of a constant period of rotation is to select a hysteresis synchronous motor. Such a motor has the property that it remains in phase with the alternating current that drives it. Thus, the problem of maintaining a constant period of rotation for the motor is reduced to the problem of making a stable alternating current power source. The motor selected was a single phase two-pole hysteresis synchronous motor specified for 115 VAC operation

at 500 Hz (manufactured by the F. C. Globe Co., Dayton, Ohio). During operation inside the vacuum system the motor's current requirement was about 0.2 A. The basic time standard for the system was a 1 MHz quartz crystal controlled oscillator. This 1 MHz signal was divided digitally to 500 Hz and fed into an active low pass filter with corner frequency ≈ 550 Hz. The low pass filter attenutated higher harmonics leaving the fundamental 500 Hz sine wave with frequency stability more than adequate to meet the 0.05% requirement stated above. The signal from the low pass filter was fed to a power amplifier which provided power for the motor.

In order to have an independent measure of the rotation period, an optical link consisting of an infrared light emitting diode and silicon phototransistor was mounted in such a way that as the motor turned, the moving slits in the collector wheel allowed the optical link to be completed twice during each complete rotation. The period between successive pulses was monitored by a frequency counter operated in the period measurement mode. During a typical fifteen hour run the mean and standard deviations of the hourly readings of this period were 999.97 μsec and 0.02 μsec respectively. This clearly exceeds the stability requirements outlined above.

In addition to its primary purpose the optical link served the collateral function of providing a time signal in phase with the angle of the motor shaft. This signal was fed into an analog delay circuit and ultimately initiated the creation of a beam pulse by the parallel plate electrostatic beam chopper (Fig. 1) which operated between the two states: "beam on" (zero voltage between the plates) and "beam off" (200 volts between the plates). The primary function of the beam chopper was to remove the beam during the period when the collector disk was between it and the target — thus preventing the unwanted beam from heating the disk.

As stated above in the section on design considerations, the rotating collector was chosen to be 5.08 cm in radius. It was fabricated from a standard alloy (2024) Al sheet 0.025 cm thick. At the edge of the disk diametrically opposite each other were cut the two rectangular slits 1.11 cm radially by 0.45 cm wide that along with the fixed slits (as shown in Fig. 1) produced an approximately triangular beam pulse. The collector disks were mounted on the hub of the motor shaft and dynamically balanced by a professional balancing company (Khougaz Electrodynamic Balancing, 15960 Blythe St., Van Nuys, CA). As final preparation before use the collector was cleaned by a standard UHV procedure.[15]

3 EXPERIMENTAL PROCEDURE

The target used in this experiment was a 93% enriched, cold rolled ^{235}U metal foil 0.0025 cm thick and about 0.5 cm^2 in area obtained from Oak Ridge National Laboratory. Prior to being placed in the vacuum chamber it was dipped in 70% HNO_3 to remove most of the oxide layer (UO_2) formed by exposure to air. This etching process lasting typically two to five minutes, was followed by a distilled water wash and a final dip in acetone. Following this operation the foil was mounted in the vacuum chamber as soon as possible in order to minimize additional oxidization.

Immediately before beginning the collection of data the target was sputter cleaned with the 80 keV $^{40}Ar^+$ beam. The d.c. current used during the cleaning run was about 3 μA, which for a sputtering yield of 2 (Gregg and Tombrello[16]) removed approximately 20 atomic layers of ^{235}U. During the sputter cleaning one of the slits in the collector was aligned with the fixed slits, thus allowing the beam to pass while preventing any ^{235}U from hitting

the collector surface. During the actual run the rate of arrival of Ar^+ ions at the target was about 5.6×10^{12} cm^{-2} sec^{-1}. This flux is sufficient to remove a monolayer from the target about every 120 sec. The pressure of the target chamber during Ar^+ bombardment was about 4×10^{-8} Torr; however, most of this was contributed by the Ar introduced by the beam. The chamber pressure without the beam present was about 4×10^{-9} Torr. It is assumed that this represents the partial pressure of the gases that would be likely to contaminate the surface during the run. Even if these gases stuck to the target with 100% probability the Ar bombardment would keep the target clean.

The pressure in the motor chamber during the run was about 2×10^{-5} Torr. It should be noted, however, that the presence of the fixed slit provided a considerable pumping impedance between the motor chamber and the in-line cold trap so that virtually all of the flight path of the ^{235}U particles was in a region assumed to be at a much lower pressure. Under the conditions described, the accumulation of the data for one pair of spectra required a continuous run of approximately fifteen hours. Following the completion of the run the collector wheel was removed from the vacuum chamber and cut into six segments. These segments of the rim were placed in contact with mica sheets which were used as the fission fragment track detectors (Gregg et al.[17]).

The collectors and detectors were then subjected to a neutron fluence, Φ, of about 10^{16} cm^{-2} in the core of the UCLA research reactor. The probability, $\sigma\Phi$, that a randomly selected ^{235}U atom, will fission under these conditions is about 6×10^{-6}. (σ is the fission cross section.) When a fission does occur, one of the energetic fission fragments enters the mica detector and penetrates approximately 10 μm causing a substantial amount of radiation damage along its path.

After the irradiation was completed and time allowed for the radioactivities produced in the irradiation to die away (about five days) the mica detectors were etched for 10 minutes in 48% HF. This acid preferentially attacks the regions of radiation damage caused by the energetic fission fragments and produces a visible pit, or track, at the site of each fission fragment penetration. These tracks were magnified and counted as a function of position on the detector. Since the track density (in tracks/cm^2) is strictly proportional to the density of collected ^{235}U atoms, the number of ^{235}U atoms per unit area was then obtained as a function of position. Counting was done at a magnification of 450 x. At this magnification a single microscope field of view was 3.6×10^{-4} cm^2. At the peak of the arrival time distribution one such field of view contained about three hundred tracks. Four fields were counted to obtain each data point on a given spectrum. In order to minimize any error caused by imperfections or flaking of the mica, two spectra, accumulated simultaneously, have been combined to give the results presented below. Because of the small probability that any given ^{235}U nucleus will fission during neutron exposure the Poisson distribution correctly describes the distribution of the number of tracks counted in any field of view about the theoretical mean. As a result, if N tracks are counted for a given data point, the error assigned is $\sqrt{N}$. The limit of resolution proved to be the natural uranium impurity level in the aluminum collector. This impurity, estimated to be about 0.5 ppm U of natural isotopic abundance, caused a background of about 15-20 tracks per field of view and limited the useful lower limit of the range of the spectrum to about 1 eV where after background subtraction the statistical error was about 60%. The uranium in the mica track detector, Indian ruby mica, contributed only about one track per field of view to the background.

4 DATA AND DISCUSSION

Figure 2 shows the measured distribution, N(z), of sputtered ^{235}U fission tracks as a function of the dimensionless variable z. z may be thought of either as the arrival time in units of 28 μsec or as the position on the rim of the collector in units of the slit width (d = 0.447 cm) and for this reason turns out to be a very convenient variable. The distinct peak at an arrival time of about 112 μsec corresponds to a velocity of 7.26×10^5 cm/sec. The error bars shown are statistical. Each point in the peak represents over two thousand counted tracks. Apart from the single peak the spectrum is apparently devoid of structure. It is interesting to consider this spectrum in the light of the random collision cascade model for the sputtering process. First, however, it is necessary to consider in greater detail the operation of the spectrometer itself in order to be able to recognize any aberrations that the measurement process might have introduced.

4.1 Mathematical Analysis of the Spectrometer

An ideal time-of-flight spectrometer differs from any practical device in two ways. In the ideal spectrometer beam pulses can be very short, that is, Dirac delta functions of time. Further, the width of the slit that defines the particles that are collected can be vanishingly narrow. This is equivalent to saying that the correspondence between location on the collector and velocity of the particles that can strike there is unambiguous. In fact, neither of these conditions can be met in a real apparatus. The purpose of the following discussion is to assess quantitatively the effect of finite pulse and slit widths on the spectrum obtained.

Because it is common in the literature of sputtering to consider energy distributions rather than velocity or arrival time distributions we shall take

as the starting point of this discussion the sputtering yield per unit energy per unit solid angle, $S(E,\Theta)$, where the angle Θ is measured from the normal to the surface being sputtered. For the geometry of the spectrometer being considered here $\Theta = 0$ because the collection solid angle is in the direction of the incident beam from the target and the target plane is chosen to be perpendicular to the beam. Define, therefore $S(E,0) \equiv S(E)$. Now since the collector is located a distance ℓ from the target the number of particles arriving per unit area in the energy range dE about E is $\varphi(E)$ and

$$\varphi(E) = \ell^{-2}\, S(E)$$

If the beam particle that gives rise to these sputtered particles strikes the target at $t = 0$ then the energy of a particle of mass m is related to its arrival time at the collector by

$$E = \tfrac{1}{2}\, m\, \left(\frac{\ell}{t}\right)^2 \qquad (7)$$

This relation may be used to change variables in the expression for $\varphi(E)$. Thus

$$\varphi'(t) = \ell^{-2}\, S[E(t)]\left|\frac{dE(t)}{dt}\right| \quad . \qquad (8)$$

This quantity $\varphi'(t)$ is the flux of sputtered particles per incident particle at time $t' = 0$ that arrives at the collector. For a beam pulse of finite duration the total flux at time t, is given by the convolution

$$g(t) = \int_{-\infty}^{t} f'(t')\varphi'(t - t')dt' \quad . \qquad (9)$$

where $f'(t')$ is the intensity of the beam at time t'. The density of particles at any location y on the wheel, $p(y)$, is the integral

of this flux over the finite time period that the point is exposed by the slit, that is from

$$t_1 = \frac{y - \frac{1}{2}d}{u} \qquad \text{to} \qquad t_2 = \frac{y + \frac{1}{2}d}{u} \ , \tag{10}$$

where u is the linear velocity of the collector at the rim. Hence,

$$p(y) = \int_{\frac{y - \frac{1}{2}d}{u}}^{\frac{y + \frac{1}{2}d}{u}} dt \int_{-\infty}^{t} f'(t')\varphi'(t - t')dt' \ . \tag{11}$$

As mentioned before, it is convenient to measure y in units of the slit width. $d = 2\pi rf$. That is

$$y = zd$$

and

$$p(z) = \int_{(z - \frac{1}{2})\frac{d}{u}}^{(z + \frac{1}{2})\frac{d}{u}} dt \int_{-\infty}^{t} f'(t')\varphi'(t - t')dt' \ . \tag{12}$$

It is also convenient to measure time in units of 1/2 the pulse width $t_0 = fT$. So $t = xt_0$ (where the primed functions f' and φ' become unprimed ones on change of variables). This change yields

$$p(z) \int_{(z - \frac{1}{2})\frac{d}{ut_0}}^{(z + \frac{1}{2})\frac{d}{ut_0}} dx \int_{-\infty}^{x} f(x')\varphi(x - x')dx' \ . \tag{13}$$

Finally, note

$$\frac{d}{ut_0} = \frac{2\pi r}{uT} = 1. \tag{14}$$

Thus, the final expression for the density of collected sputtered material becomes

$$p(z) = \int_{z-\frac{1}{2}}^{z+\frac{1}{2}} dx \int_{-\infty}^{x} f(x')\varphi(x-x')dx' \quad . \tag{15}$$

In this experiment the pulse shape was approximately triangular and centered at t = 0. Thus,

$$f(x) = \begin{cases} 1 - |x|, & |x| \leq 1 \\ 0 , & |x| > 1 \end{cases} , \tag{16}$$

is the normalized pulse shape. Let us now consider a specific example of this formula.

4.2 Random Collision Cascade Model

The random collision cascade model proposed by Thompson[6] gives an expression of the following form for $S(E,\Theta)$,

$$S(E,\Theta) = \frac{2}{\pi} S \left[\frac{EU}{(E+U)^3}\right] \cos\Theta \tag{17}$$

where S is the total sputtering yield and U is a surface binding energy which is usually taken to be the sublimation energy. The presence of this surface binding gives this spectrum its characteristic peak at a value of U/2 and is responsible for its linear decrease to zero at low energies. For our experimental configuration and the spectrum given by Equation (17):

$$\varphi(x) = \left(\frac{S}{\pi \ell^2}\right) \frac{4 x_0^{\,4} x}{(x^2 + x_0^{\,2})^3} \equiv \frac{S}{\pi \ell^2}\, \lambda(x, x_0) \tag{18}$$

where

$$x_0^{\,2} = \frac{\frac{1}{2} m (\ell / t_0)^2}{U} \equiv \frac{E_0}{U}\,, \tag{19}$$

m = mass of sputtered particle,

t_0 = fT = 28 μsec,

T = rotation period = 2 ms,

ℓ = target-collector distance = 81.3 cm,

and U = surface binding energy of ^{235}U.

This defines the function λ. x_0 may be thought of as the time (in units of t_0) that it takes a particle of energy U to travel from the target to the collector. For our apparatus E_0 = 1040 eV. For numerical calculation it is convenient to note that particles that strike the collector at position z have energy

$$E = \frac{x_0^{\,2}}{z^2}\, U = \frac{E_0}{z^2}\,. \tag{20}$$

Although tedious, it is possible to carry out the integral (15) analytically for the functions (16) and (18). The result is

$$p(z) = \frac{S}{\pi \ell^2} \left[\gamma(z, x_0) + \epsilon(z, x_0)\right] \tag{21}$$

where

$$\gamma(z, x_0) = \frac{x_0^{\,2}}{2} \sum_{n=0}^{3} (-1)^n \binom{3}{n} \left(\frac{z + n - 3/2}{x_0}\right) \tan^{-1}\left(\frac{z + n - 3/2}{x_0}\right); \quad \frac{1}{2} \le z \tag{22}$$

$$\epsilon(z,x_0) = \begin{cases} \frac{x_0^2}{2}\left[\left(\frac{z-3/2}{x_0}\right)^2 - \left(\frac{z-3/2}{x_0}\right)\tan^{-1}\left(\frac{z-3/2}{x_0}\right)\right] & ; \quad \frac{1}{2} \le z \le \frac{3}{2} \\ \\ 0 \quad ; \qquad z > \frac{3}{2} \end{cases} \tag{23}$$

Here $\binom{3}{n}$ is the binomial coefficient $\binom{3}{n} = \frac{3!}{n!(3-n)!}$

Only the region $z \geq 1/2$ is of interest since the slit in the rotating collector is located in the region $-\frac{1}{2} \leq z \leq \frac{1}{2}$. The function $\gamma(z,x_0) + \epsilon(z,x_0)$ is the spectrum that would be obtained by the spectrometer used in this experiment if an hypothetical ideal spectrometer obtained $\lambda(z,x_0)$. The two expressions $\gamma(z, 13.9) + \epsilon(z, 13.9)$ and $\lambda(z, 13.9)$ are plotted in Figure 3. Over the entire range of z the two curves are practically indistinguishable. The value $x_0 = 13.9$ is chosen on the basis of a sublimation energy of U = 5.4 eV (Gschneidner[18]). The conclusion that can be drawn from Figure 3 is that the spectrometer does not introduce systematic error into the measurement in spite of its non-ideal nature.

Note that there is qualitative agreement between the random collision cascade model, Figure 3, and the data, Figure 2, but that the data peak at a smaller z (higher velocity) than expected.

4.3 The Energy Spectrum

If $p(z)$ is an arrival time spectrum measured on an ideal spectrometer then the corresponding energy distribution is given by the inverse of (8).

$$S(E) = \ell^2 p[z(E)] \left|\frac{dz(E)}{dE}\right| . \tag{24}$$

Since

$$E = \tfrac{1}{2} m \left(\frac{\ell}{t_0}\right)^2 \frac{1}{z^2} = E_0 z^{-2} , \tag{25}$$

Parametric equations for S(E) are

$$S(E) = \frac{\ell^2 z^3}{2 E_0} p(z) , \qquad \text{where} \qquad E = \frac{E_0}{z^2} . \tag{26}$$

We have seen how the deviation from ideal behavior of the spectrometer alters the arrival time distribution. In order to judge the systematic error in inferring S(E), for a non-ideal spectrometer the distribution $p(z) = \ell^{-2}[\gamma(z,13.9) + \epsilon(z,13.9)]$ has been inverted according to (26). Let S'(E) be the result of this process. The true S(E) that leads to this p(z) is known to be Equation (17) with $(S/\pi) \cos \Theta = 1$. S'(E) is plotted as the dashed curve in Figure 4. Over the entire range shown S'(E) differs from S(E) by less than the width of the line. Clearly, it is reasonable to take

$$S(E) = S'(E) . \tag{27}$$

The result of inverting the data according to Equation (26) is also shown in Figure 4 as a collection of data points with statistical error bars. The data clearly do not fall off as fast as E^{-2} at higher energies. In fact, a power curve fit to points above $\approx$ 200 eV indicates that the behavior is about $E^{-1.77}$. For this reason the data were fitted with a curve of the form

$$S(E) = A \frac{E}{(E + B)^{2.77}} , \tag{28}$$

where A is simply a constant scale factor. The final (smooth) curve in Figure 4 is this function. A value of B = 5.4 eV (the sublimation energy) was found to give a quite adequate fit. A was taken to be 3.83 for normalization. It should be stressed that this curve is intended only to summarize the data and that no theoretical significance is necessarily associated with it.

The most obvious sources of possible error in this experimental arrangement are attenuation of particles in flight by collision with the residual gas and the sticking probability of ^{235}U atoms that strike the Al collector. Thompson et al.[10] found that for gold incident on steel the sticking probability was about unity independent of energy. Results obtained in this laboratory indicate that for ^{235}U on aluminum the effective sticking probability integrated over all energies of interest in the sputtering measurements exceeds 97% (Griffith et al.[19]).

In order to estimate the attenuation of the sputtered particles by the residual gas in the vacuum system a test was conducted in which collectors were placed 80.2 cm and 25.8 cm away from the ^{235}U target. On the basis of geometry alone the ratio of track densities obtained on these collectors should be .103. In order to simulate the conditions during a velocity spectrum measurement, the sputtering was done at a pressure in the target area of $\approx 2 \times 10^{-8}$ Torr. Track densities obtained on the near and far collectors were 1.87×10^{6} tracks/cm^2 (±3%) and 1.90×10^{5} tracks/cm^2 (±3%), respectively, giving a ratio of .102, essentially equal to the value predicted on the basis of geometry alone. (Even at a pressure of 3×10^{-6} in the target area, a deficit in the ratio of track densities of only 19% was observed.) These data suggest that aberrations introduced by this effect are minimal. As a further check on the consistency of this result an estimate of the sputtering yield, S, on the basis of the track density on the near collector was made. A value of 2 ± 1 was obtained in agreement with the value obtained by Gregg and Tombrello.[15] (The large error in this number arises from uncertainties in the absolute magnitude of the neutron fluence and argon beam charge integration. Note, however, that neither of these possible errors affects either the energy spectrum or attenuation measurement since both are relative measurements.)

5 SUMMARY

A mechanical time-of-flight spectrometer has been constructed and used in conjunction with the nuclear track technique for ^{235}U detection to measure the energy spectrum of sputtered ^{235}U from a polycrystalline ^{235}U metal target. A spectrum peaking in the range 2-4 eV and decreasing approximately as $E^{-1.77}$ at energies above $\approx$ 100 eV has been found. The sensitivity of the nuclear track technique suggests that it will be possible in future experiments not only to study the behavior of the spectrum under changes in the bombarding ion and its energy but also to examine the energy spectrum of ^{235}U ejected in the sputtering of various uranium compounds, alloys or minerals.

The authors wish to thank D. S. Burnett, J. E. Griffith, R. Gregg and S. Streight for many useful discussions during the course of this work and also to express appreciation to F. Meulemans, W. Schick, and D. Wasserburg who aided in the apparatus construction and data taking.

REFERENCES

1. G. M. McCracken, Rep. Prog. Phys. 38, 24 (1975).
2. R. V. Stuart and G. K. Wehner, J. Appl. Phys. 35, 1819 (1964).
3. R. V. Stuart, G. K. Wehner and G. S. Anderson, J. Appl. Phys. 40, 803 (1969).
4. H. Oechsner, and L. Reichert, Phys. Lett. 23, 90 (1966).
5. F. Bernhardt, H. Oechsner and E. Stumpe, Nucl. Instr. Methods 132, 329 (1976).
6. M. W. Thompson, Phil. Mag. 18, 377 (1968).
7. B. W. Farmery and M. W. Thompson, Phil. Mag. 18, 415 (1968).
8. G. E. Chapman, B. W. Farmery, M. W. Thompson and I. H. Wilson, Rad. Eff. 13, 121 (1972).
9. I. Reid, B. W. Farmery and M. W. Thompson, Nucl. Instr. Methods 132, 317 (1976).
10. M. W. Thompson, B. W. Farmery and P. A. Newson, Phil. Mag. 18, 361 (1968).
11. H. Beuscher and K. Kopitzki, Z. Physik 184, 382 (1965).
12. E. Hulpke and C. H. Schlier, Z. Physik 207, 294 (1967).
13. J. Politiek and J. Kistemaker, Rad. Eff. 2, 129 (1969).
14. P. K. Haff, Z. E. Switkowski, D. S. Burnett and T. A. Tombrello, Proc. VIII Lunar Sci. Conf. (1977) in press.
15. A. Roth, Vacuum Technology (North Holland, Amsterdam, 1976) p. 337.
16. R. Gregg and T. A. Tombrello, submitted to Rad. Eff. (1977)
17. R. Gregg, Z. E. Switkowski and T. A. Tombrello, Nucl. Instr. Methods (1977) in press.
18. K. A. Gschneidner, Jr., Solid State Physics 16, 275 (1964).
19. J. Griffith, R. A. Weller, S. Streight and T. A. Tombrello, to be published.

FIGURE CAPTIONS

Fig. 1. Schematic diagram of the apparatus described in the text. A collector wheel (upper left) is also shown. The wheel's diameter is 10.16 cm, and the slits in the rim are .45 × 1.11 cm.

Fig. 2. The average number of tracks per area cm^2, $N(z) = \sigma\Phi p(z)$, is plotted as a function of position on the collector, z (measured in units of the slit width d = .447 cm). The representative error bars shown are statistical.

Fig. 3. The functions $[\gamma(z,13.9) + \epsilon(z,13.9)]$ (smooth curve) and $\gamma(z,13.9)$ (crosses) that describe the predicted result of measuring a spectrum $E/(E+5.4)^3$ with the instrument used in this experiment and an hypothetical ideal spectrometer, respectively. The excellent agreement indicates that systematic error introduced by the measuring process is small.

Fig. 4. The energy spectrum, S(E) in arbitrary units, of sputtered ^{235}U inferred from the data of Fig. 1. Error bars are statistical. The smooth curve is an empirical fit to the data (see text). The dashed curve is the function $6.5E/(E+5.4)^3$ (Ref. 6). Note that the vertical scale is arbitrary, and the curves have been normalized to agree near the peak.

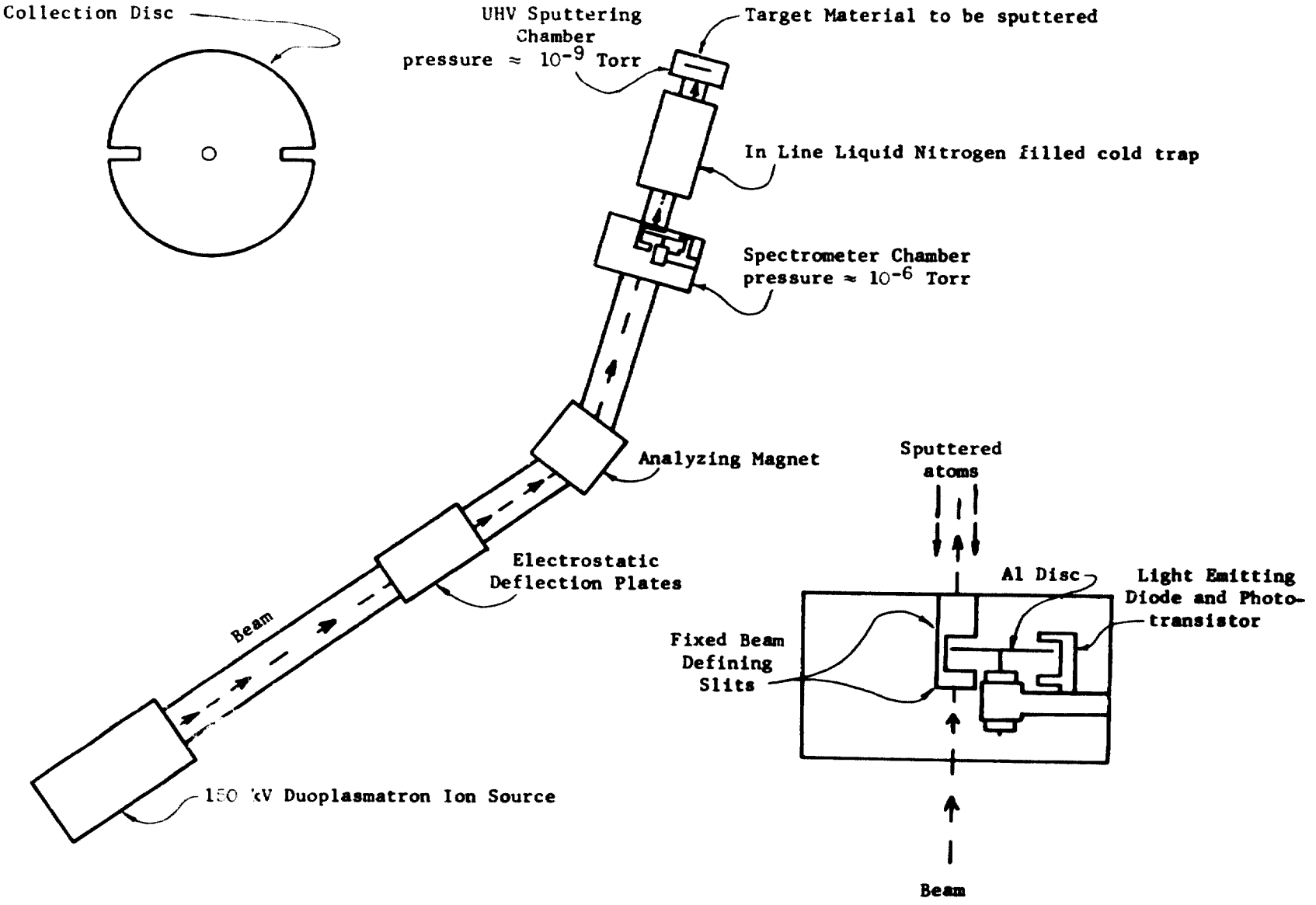
Collection Disc
UHV Sputtering Chamber pressure ≈ 10^{-9} Torr
Target Material to be sputtered
In Line Liquid Nitrogen filled cold trap
Spectrometer Chamber pressure ≈ 10^{-6} Torr
Analyzing Magnet
Electrostatic Deflection Plates
Beam
150 kV Duoplasmatron Ion Source
Sputtered atoms
Al Disc
Light Emitting Diode and Photo-transistor
Fixed Beam Defining Slits
Beam

Fig. 1

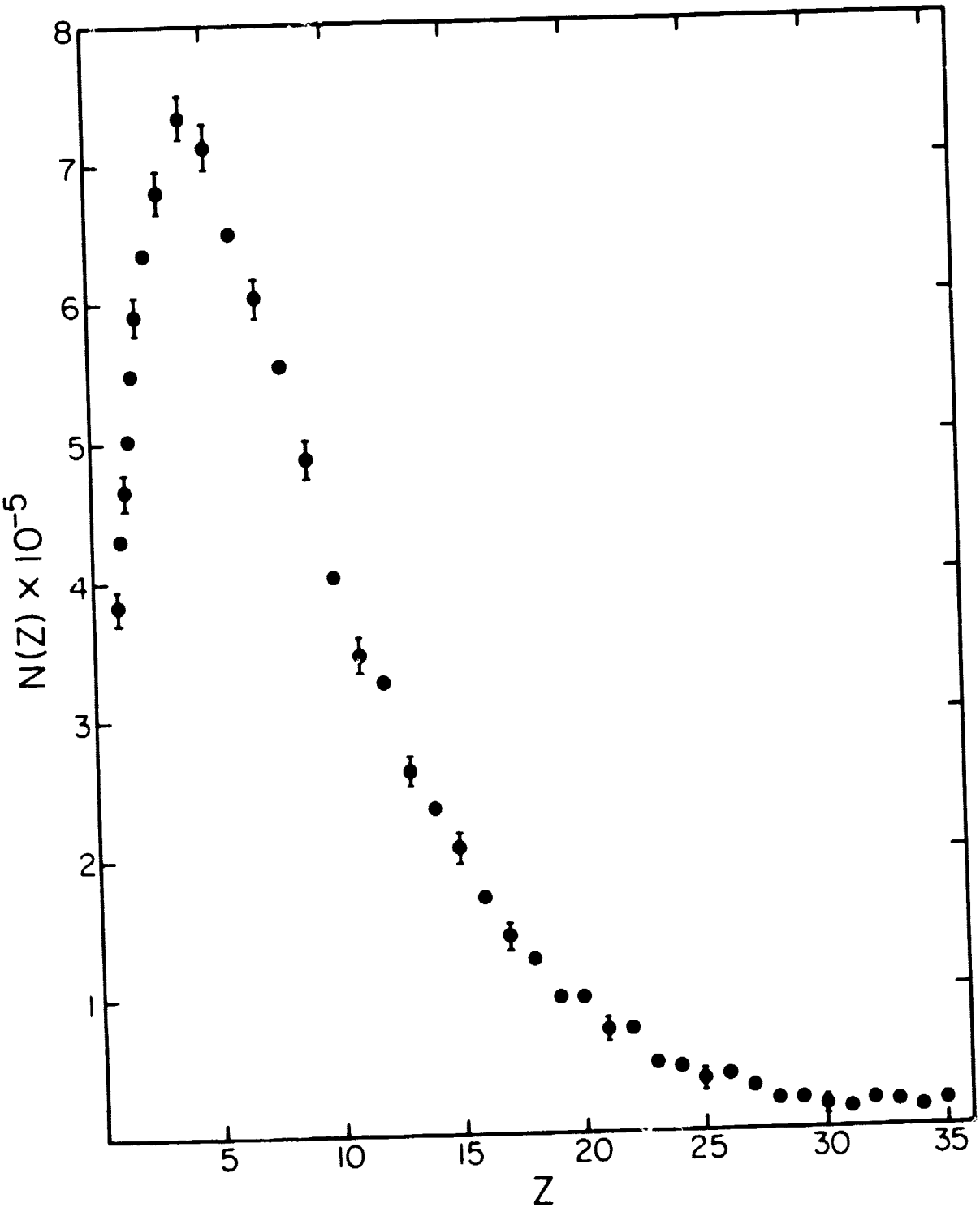

Fig. 2

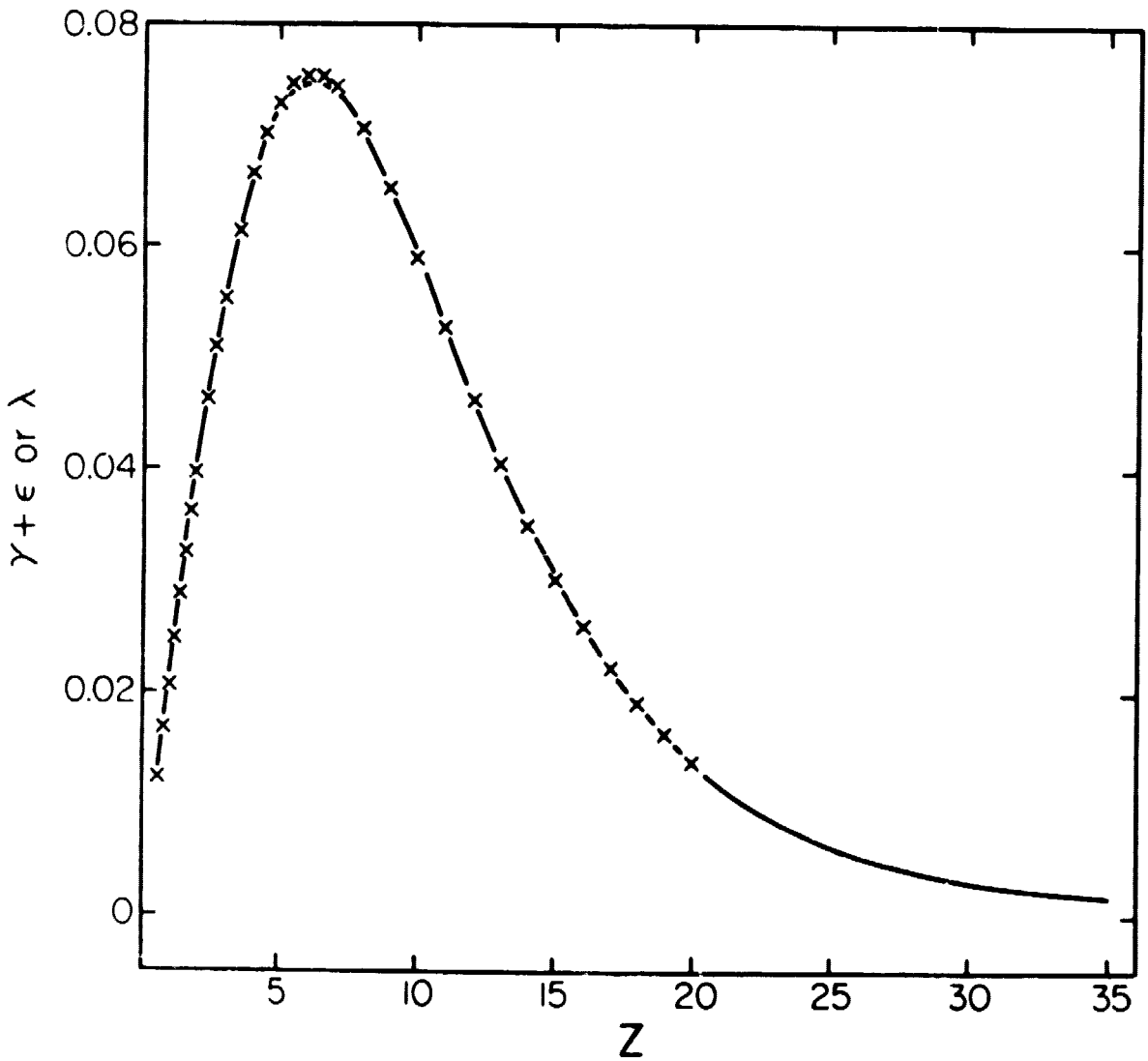

Fig. 3

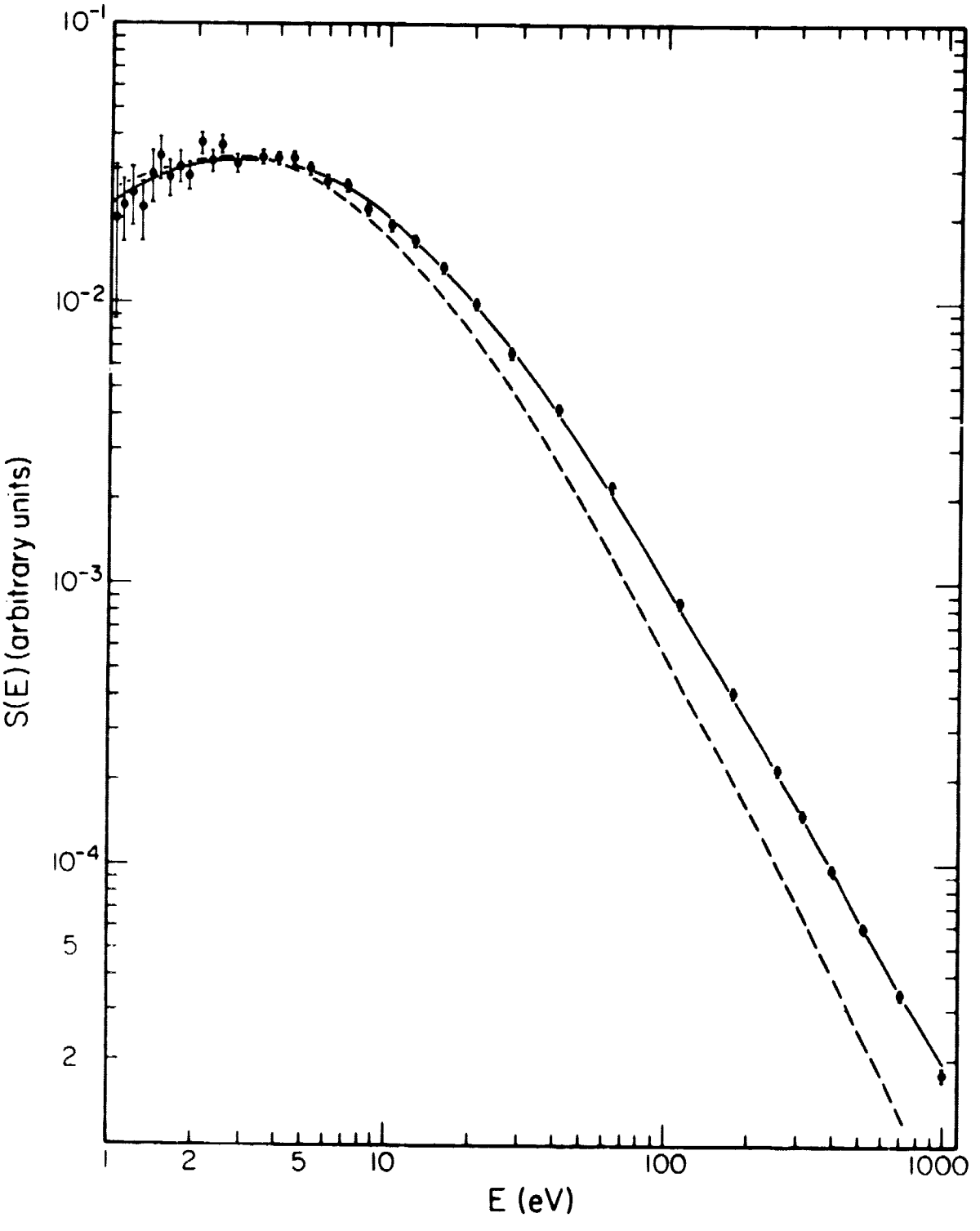

Fig. 4